Mean Value SI Engine Model for Control Studies

Hendricks, Elbert; Sorenson, Spencer C

Published in:
American Control Conference

Publication date:
1990

Document Version
Publisher's PDF, also known as Version of record

MEAN VALUE SI ENGINE MODEL FOR CONTROL STUDIES

Elbert Hendricks, Servolab. and IMSOR
Spencer Sorenson, Laboratory for Energetics,

The Technical University of Denmark
DK–2800 Lyngby, Denmark

ABSTRACT

This paper presents a mathematically simple nonlinear three state (three differential equation) dynamic model of an SI engine which has the same steady state accuracy as a typical dynamometer measurement of the engine over its entire speed/load operating range (±2.0%). The model's accuracy for large, fast transients is of the same order in the same operating region.

Because the model is mathematically compact, it has few adjustable parameters and is thus simple to fit to a given engine either on the basis of measurements or given the steady state results of a larger cycle simulation package. The model can easily be run on a Personal Computer (PC) using a ordinary differential equation (ODE) integrating routine or package. This makes the model is useful for control system design and evaluation.

1. Introduction

Mean value engine models seek to predict the mean values of the gross external engine variables (f.ex. crank shaft speed and manifold pressure) and the gross internal engine variables (f.ex. thermal and volumetric efficiency) dynamically in time. The time scale of this description is much longer than a single engine cycle and much shorter than the time required for a cold engine to warm up (1000 cycles or so). The time resolution of the model is just adequate to describe accurately the change of the mean value of the most rapidly changing engine variable.

Often mean value SI engine models found in the literature are too incompletely documented to judge their overall accuracy or are specialized to study a particular physical or control problem. In contrast to earlier efforts, the mean value SI model here is designed to be applicable to all of an engine's important subsystems over it's entire operating range. It should also to be applicable to central fuel injection (CFI), simultaneous multipoint injection (EFI) and sequential fuel injection (SEFI) engines. Moreover its accuracy is documented over the entire operating range of the engine. The model to be presented here is based on experimentally obtained data.

2. Engine Diagram

A schematic block diagram of a four–cycle CFI SI engine is presented in figure 1. This is the most difficult injection engine to model due to the fuel flow dynamics in the intake manifold. The figure shows the basic systems to be modelled: the fuel film dynamics in the intake manifold; the air mass flow past the throttle plate into the volume V, between the throttle plate and intake valves; the engine displacement volume, V_d which drives the crank shaft inertia and load dynamics.

The engine input variables are the throttle angle, α, the injected fuel flow, $\dot{m}_{fi}$, and the ignition timing angle, θ (degrees BTDC). The state

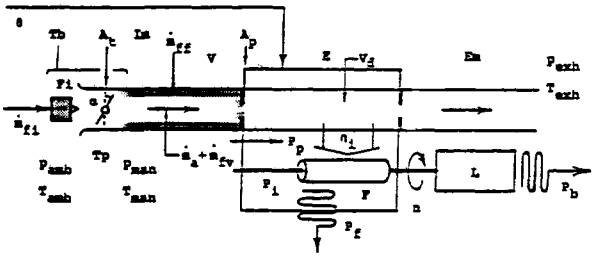

Figure 1. Schematic block diagram of a CFI engine. The different physical components of the engine are indicated by the abbreviations. These are Tb (throttle body), Fi (fuel injector), Tp (throttle plate), Im (intake manifold), E (engine), Em (exhaust manifold), F (engine internal frictional losses) and L (load).

variables are the fuel film mass flow, $\dot{m}_{ff}$, the crank shaft speed, n, and the absolute manifold pressure, p_{man}. Gross internal engine variables such as the thermal and volumetric efficiencies are to be modelled and determined as functions of the state variables. The engine load (power or torque) in this work is considered as a disturbance of the engine. The engine is to be modelled in the open loop.

3. Modelling Philosophy: Time Scaling

In a mean value engine model there are two basic kinds of relationships between engine variables: instantaneous and time developing. The difference between the two types of relationships is the relative time scale on which the relevant subsystems respond physically. Instantaneous relationships are those in which equilibrium is established in the course of one or a few engine cycles: these are algebraic equations. A time developing relationship between engine variables is one which takes between 10 and 1000 engine cycles to reach equilibrium: these become differential (or state) equations.

The instantaneous subsystem equations must be as simple as possible without doing violence to physical reality. Such equations contain a minimum of fitting parameters and facilitate global fitting accuracy.

3.1 Time Developing Engine Relations: System State Equations. The fuel flow together with the air flow constitute the input energy flow to the engine while the energy output is the load power plus the frictional and pumping losses. These three state equations can all be derived from conservation of mass or energy applied to these three subsystems.

A simple submodel for the fuel dynamics has been suggested in [1]. In this submodel the fuel flow consists of two contributions: a fuel vapor flow and a fuel film flow. The intake manifold is assumed to by heated by the engine coolant. The fuel vapor reaches the engine port together with the air flow within an engine cycle. The portion

of the total fuel flow which becomes the fuel film in the manifold is evaporated off the heated intake manifold with a time constant, τ_f. The two components then combine to become the fuel flow into the engine's intake valves. The fraction of the fuel flow which strikes the manifold and becomes fuel film is X while that which becomes fuel vapor is 1–X. At a given manifold temperature X is a function of the throttle angle, α, in a CFI engine. In EFI and SEFI engines, the injector is just above the intake port and X is approximately constant and independent of the throttle angle at a given engine coolant temperature. The simplified model can be expressed in equation form as

$$\dot{m}_{fv} = (1 - X)\dot{m}_{fi} \qquad (1)$$

$$\dot{m}_{ff} = (1/\tau_{ff})(-\dot{m}_{ff} + X\dot{m}_{fi}) \qquad (2)$$

$$\dot{m}_f = \dot{m}_{fv} + \dot{m}_{ff} \qquad (3)$$

The block diagram of the fueling dynamics is on the top of figure 5. The fueling submodel above is clearly a very simplified view of the complicated physical processes which in reality govern the flow of fuel in the manifold. Nevertheless this model can be shown to represent the fuel flow dynamics sufficiently accurately for use in the engine model[2]. As it is impractical to measure $\dot{m}_f$ directly, equations (1), (2) and (3) in general represent a very unpleasant control problem which can only be solved by feedforward or advanced control algorithms.

The rate of change of rotational kinetic energy of the crank shaft is equal to the fuel power available to accelerate the crank shaft, its associated moment of inertia, and that of the load, minus the losses.

$$\dot{n} = -\frac{(P_f + P_p + P_b)}{(I\ n)} + \frac{H_u \eta_i \dot{m}_f(t-\tau_d)}{(I\ n)} \qquad (4)$$

where the units of I have been selected to give a convenient form of the equation in terms of n. Thus $I = ((2\pi/60)^2/1000)(I(\text{engine})+I(\text{load}))$, where I(...) is the moment of inertia of the engine or the load. $\dot{m}_f(t-\tau_d)$ indicates that there is a time delay τ_d between the edge of a fuel flow step at the engine intake valves and the increase (or decrease) of engine speed. The time delay can be approximated as the mean time between mixture ignitions and is for a four cycle engine

$$\tau_d = \frac{2\pi}{n_{cyl}(2\pi n/60)} = \frac{1}{2}\frac{60}{n_{cyl}n} \qquad (5)$$

where n_{cyl} is the number of cylinders. The block diagram of equation (4) is in the middle of figure 5.

The state equation for the manifold pressure is obtained by applying conservation of mass to the volume V of figure 1. The manifold pressure state equation can be found to be

$$\dot{p}_{man} = -\frac{n\ V_d}{120\ V}\eta_{vol}\ p_{man} + \frac{RT_{man}}{V}\dot{m}_{at}(\alpha,\ p_{man}). \qquad (6)$$

Equation (6) is diagramed on the bottom of figure 5.

Equations (1), (2), (3), (4) and (6) are the state equations of the SI mean value engine model.

3.2 **Instantaneous Engine Variables.** The algebraic functions for the instantaneous internal engine variables are determined from steady state measurements. Thus functional forms must be found for X in equations (1) and (2), for P_f, P_p, P_b and η_i in equation (4) and η_{vol} and $\dot{m}_{at}$ in equation (6). The main tool for this is nonlinear regression analysis and carefully measured engine data.

The variable X and parameter τ_f in equations (1) and (2) represent a special case in this work. It is not possible to determine them from steady state engine measurements. To find these internal variables accurately it was necessary to apply statistical identification techniques (Maximum Likelihood method and Kalman filtering) because of the noise level (see [2]). The function which was found for $X(\alpha)$ for a CFI engine is approximately

$$X(\alpha) = 1-\cos(a(\alpha-\alpha_0)) \qquad (7)$$

where a is a constant and where α_0 is the throttle angle when the throttle is closed. If it is desired to extend the model to another temperature range or engine type then a large selection of work is reported in the literature (see [3]).

In the shaft speed state equation there are four functions which must be found in order to integrate the differential equation: these are the various power expressions and the thermal efficiency.

Friction and pumping losses in an engine can together be expressed as polynomials in the shaft speed and the intake and exhaust manifold pressures[4]. The approximate expression used in the model is

$$P_f + P_p = n(a_0 + a_1 n + a_2 n^2) + n(a_3 + a_4 n)p_{man} \qquad (8)$$

It is possible to split the thermal efficiency into four more or less independent effects. One is lead to seek an expression of the form

$$\eta_i(\theta,\ \lambda,\ n,\ p_{man}) = \eta_i(\theta,\ n)\cdot \eta_i(\lambda,\ n)\cdot\eta_i(n)\cdot\eta_i(p_{man}) \qquad (9)$$

All of these factors can be measured from steady state mapping data if the proper experiments are made. Figure 2 shows thermal efficiency data obtained for a 1.1L Ford CFI engine plotted as a function of the engine speed. The dominant n dependence can be modelled physically by considering the coolant heat losses. One finds an expression for $\eta_i(n)$ which is

$$\eta_i(n) = \eta_{io}(1 - \eta_{i1}\ n^{-b}) \qquad (10)$$

where η_{io} is approximately the efficiency of an ideal Otto engine ($\simeq 0.45$), η_{i1} is a constant and b $\simeq 0.2$. The function $\eta_i(p_{man})$ gives only a slight perturbation of the main functional dependence given of equation (10). Its effect only amounts to 1 or 2% and the form was found to be a parabola in p_{man} independent of n. It was determined as

$$\eta_i(p_{man}) = p_{m0} + p_{m1}p_{man} + p_{m2}p_{man}^2 \quad (11)$$

where p_{m0}, p_{m1} and p_{m2} are constants. The equations which were found for the last two contributions to η_i are given below.

$$\eta_i(\theta, n) = \Theta_0 + \Theta_1(\theta - [\Theta_2 n + \Theta_3])^2 \quad (12)$$

where the Θ's are all constants. The equation has been written in this form to emphasize it's simple geometry. Similarly to the spark advance dependence the function $\eta_i(\lambda, n)$ can be modelled as a parabola close to a stoichiometric operating point, in the range of about $0.7 \leq \lambda \leq 1.2$.

$$\eta_i(\lambda,n) = \Lambda_0 + \Lambda_1\lambda + \Lambda_2\lambda^2 + \Lambda_3 n \quad (13)$$

where the Λ's are constants. The n dependence in both equations is weak but significant.

The manifold pressure state equation contains two important instantaneous variables which must be modelled: the volumetric efficiency and the air mass flow past the throttle plate. The functional dependence of the volumetric efficiency based on manifold conditions is

$$\eta_{vol} = \eta_{vn0} + \eta_{vn1}n + \eta_{vn2}n^2 + \eta_{vp1}p_{man} \quad (14)$$

The n and p_{man} dependencies are decoupled so that this is a simple parabolic surface in n with a constant gradient in p_{man}. In order to check the regression equation (14) (after it was fitted to the experimental data and tested), it was first referred to ambient conditions via the relation, $\rho_{amb}\,\eta_{vamb} = \rho_{man}\,\eta_{vol}$ (where the rho's are the relevant air densities). The experimental points were then plotted along with the transformed regression equation. In addition η_{vamb} was calculated using an engine cycle simulation program due to one of the authors[5]. The results are given on figure 3. The agreement of the predictions of both the regression equation and the cycle simulation with the experimental data is quite good.

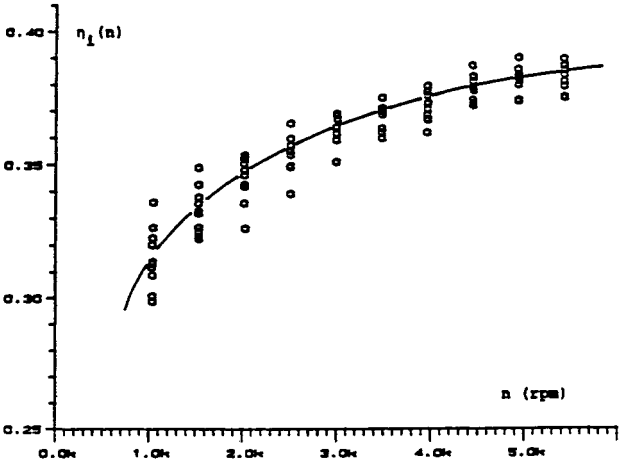

Figure 2. Thermal efficiency data on the Ford 1.1L engine plotted against n. Though it cannot be seen, the manifold pressures are a parabola in the dimension going into the paper, though a very shallow one.

It is by now well known that the air mass flow past the throttle plate, $\dot{m}_{at}$, can be closely approximated as the air mass flow of a compressible fluid through a converging nozzle with an effective area $A_t = (\pi/4)\,D^2$. In its simplest form this equation can be written

$$\dot{m}_{at}(\alpha, p_{man}) = c_t \frac{\pi}{4} D^2 \frac{p_{amb}\sqrt{\kappa'}}{\sqrt{RT_{amb}}} \beta_1(\alpha)\ \beta_2(p_{man}) + \dot{m}_{at0} \quad (15)$$

where c_t, D, p_{amb}, R, T_{amb}, and $\kappa' = 2\kappa/(\kappa - 1)$ are physical constants and $\dot{m}_{at0}$ is a fitting constant. The functions β_1 and β_2 are given by

$$\beta_1(\alpha) = 1 - \cos(\alpha - \alpha_0),$$

$$\beta_2(p_{man}) = \begin{cases} \sqrt{p_r^{\frac{2}{\kappa}} - p_r^{\frac{\kappa+1}{\kappa}}}, & \text{if } p_r \geq \left[\frac{2}{\kappa+1}\right]^{\frac{\kappa}{\kappa-1}} \\ \sqrt{\left[\frac{1}{\kappa'}\right]\left[\frac{2}{\kappa+1}\right]^{\frac{\kappa+1}{\kappa-1}}}, & \text{otherwise} \end{cases} \quad (16)$$

where $p_r = p_{man}/p_{amb}$ (see [4]) and α_0 is a constant. In the second case of course the air flow is sonic. $\dot{m}_{at0}$ is the bypass air mass flow. This equation assumes that the effective throttle area is given by $\frac{\pi}{4} D^2 (1 - \cos(\alpha - \alpha_0))$ which is only an approximation. The true physical throttle area is actually a much more complicated expression (see [3]) and in some cases it may be necessary to use a more exact expression.

Considering the influences of measurement

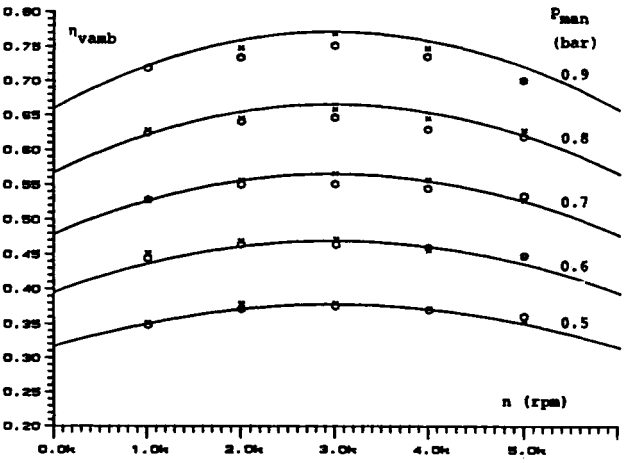

Figure 3. The volumetric efficiency based on the ambient pressure plotted against the crank shaft speed with the manifold pressure as a parameter. The x's are experimental points while the circles are points calculated with a cyclic simulation routine (FLOSIM). The fully drawn curves are those generated by equation (14) when used to fit η_{vamb}.

noise and secondary (unmodelled) physical effects it was thought that equation (15) would provide sufficient accuracy for the purpose at hand. To check this assumption the air mass flow to a 1.1L Ford engine was plotted against the parameter $\beta = \beta_1 \cdot \beta_2$ for a large series of operating points distributed over the engine's entire practical operating range. These results are shown in figure 4. It may be observed that the dependence on the parameter β is linear (diagonal curve). Thus equations (15) and (16) are good approximations to the air mass flow past the throttle plate under normal circumstances.

It will have been noticed that there are a number of experimental points on horizontal curves not described by equation (15). These points are especially encountered at low engine speeds and large throttle angles. In these cases, the air flow is independent of the parameter β. The physical explanation for this is that for low flow rates, the throttle plate is only an effective flow restriction for small throttle angles. The air flow is then determined by the engine speed alone. It is not difficult to include this operating region in the if this is desired.

A block diagram of the overall nonlinear mean value engine model is on figure 5. There are feedback boxes around each integrator which contain time constants, τ_f, τ_m and τ_{man}. These are the large signal time constants of the engine. These are not the same as the small signal time constants of conventional linear systems but are related to them. The expressions for the large signal time constants are τ_f = constant, $\tau_m = \frac{I}{k_b\, n}$, $\tau_{man} = \frac{120V}{n\ \eta_{vol}\ V_d}$. To give an idea of the magnitude of the large signal time constants one can consider a typical 1 – 1.5L engine. For such an engine with I = 0.5 kg m² at 5000 rpm, delivering 50 kW: $\tau_f \simeq 0.25 - 0.5$ sec at 20°C, $\tau_m \simeq 2.74$ sec, and $\tau_{man} \simeq 17$ msec. The mean value engine model thus suggests that an engine is a stiff system: the ratio of it's eigenfrequencies is very large.

4. Model Verification

In order to judge the accuracy of the model in the steady state, the mean and standard deviations of the errors in the model's predictions were calculated for 100 mapping points for a Ford 1.1L CFI engine. The results are shown in table 1 below. The power range is from idle load (Pi ≃ 1 kW) to full load (≃ 45 kW) and the speed range is idle to 6000 rpm.

(% error)	mean error	error std. dev.
n	0.35	1.80
p_{man}	–0.27	1.15
$\dot{m}_a$	0.28	1.90
η_i	0.07	1.70
η_{vol}	–0.15	1.10

Table 1: Mean errors and standard deviations (in percent) in the steady state predictions of the mean value engine model for key internal and external engine variables.

In the table it can be seen from the small mean errors that the variable estimates are central. The standard deviations are a measure of the actual error in the model and in all cases are quite small. Errors of the order quoted are of the same magnitude as the experimental uncertainty itself. This implies that table 1 is showing the uncertainty of the experiment and not the error in the model itself. Such a conclusion cannot however conclusively be supported without a much greater and multiply redundant mapping of the engine.

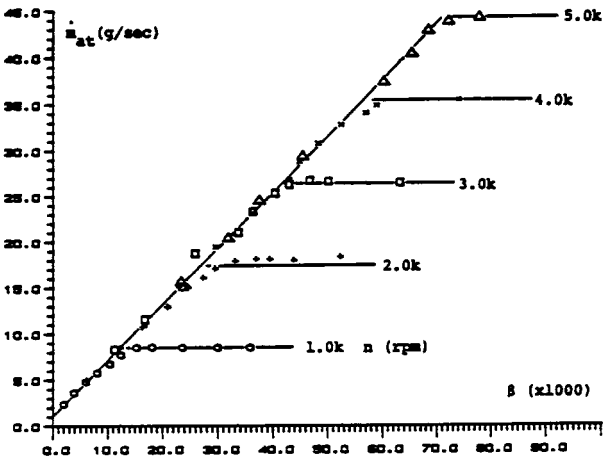

Figure 4. The throttle plate air mass flow plotted against the parameter β for a series of experiments on the 1.1L Ford engine. Notice the linear dependence on β on the diagonal of the curve. The presence of the points to the right of the diagonal is explained in the text.

It is not thought that the results of table 1 "prove" the model in any sense in spite of the clearly apparent accuracy. What table 1 does show is that with reasonable assumptions about the form of internal engine variables, the mean value model is capable of giving a mathematically consistent picture of engine operation in spite of nearly unavoidable systematic and statistical measuring errors. This is an extremely useful characteristic for such a simple model and suggests that it will be possible to fit it to most conventional SI engines with the accuracy allowed by the available experimental apparatus.

In order to collect data for the dynamic model response experiment, a set of time responses was recorded using various engine input and load excitations. The tests were performed on an eddy current dynamometer on the 1.1L Ford engine modelled above. The control system was a conventional speed–throttle digital system utilizing engine map data. It could provide acceleration enrichment though without the accuracy necessary for low emissions and ideal air/fuel ratio control (λ = 1). The main intention of the experiments was to move the engine over as large a portion of its operating range as possible, compatible with "normal operation". As the engine was being controlled by a conventional type of control strategy, this strategy played a large part in the results obtained. In particular the control system showed itself to be improperly calibrated and had a tendency to run lean. This was not important as this only provided a more complete test of the mathematical model.

The transient results which will be presented are for the engine being operated on a steep torque curve with a fast tip–in/–out throttle angle

transient. For the simulation the mean value model was provided with the measured throttle angle, injected fuel flow and load. The measurable external engine variables were logged while at the same time the exhaust air/fuel ratio was monitored for comparison with the predictions of the model. The simulation experiment is summarized in figures 6a–f.

Figure 6a shows the throttle angle step which was applied at about t = 0.5 sec. The rise time is fast: about 250 msec. This leads in figure 6b to a nearly identical manifold pressure response except for the effects of manifold filling. The manifold pressure response (1: meas.) is predicted very accurately as is the air mass flow (1: calc.) on figure 6c. Figure 6d shows the fuel mass flow produced by the control system. This signal was obtained by decoding the pulse width modulated signal used to drive the low pressure CFI fuel injector. The initial peak in the fuel response is due to the acceleration enrichment. There are some injector misfires and steps in the fuel flow due to jumps in the look–up tables. The misfiring of the injector is clearly reflected in the measured and calculated λ (see figure 6e). The misfiring of the injector at t = 0.6 and 0.8 sec is shown on the calculated response as sharp lean spikes while the measured response is somewhat smoother. This is because the λ sensor itself has a built in low pass filter while λ is calculated directly as $\dot{m}_{at}/(\dot{m}_f L_{th})$. The crank shaft speed response to the throttle angle pulse is shown on figure 6f where a small time shift is apparent due to measurement time delays. This allows the calculated response to be distinguished from the measured data.

The overall transient accuracy of the model is obviously quite good considering that the test is open loop and the mean value model and the experimental engine are running independently of each other. In particular the accuracy of the manifold pressure and air mass flow predictions is very good considering the speed and magnitude of the low to high throttle angle transition. The same accuracy has been observed during a number of equivalent experiments of different types at a number of different power levels.

5. Conclusions

A simple three state dynamic mean value model has been presented here which models a naturally aspirated four-cycle SI engine. It includes separately validated models of the most important engine subsystems. Moreover it has been globally validated in the steady state over the entire operating range of the engine to an accuracy of better than ±2.0% (for the most important internal and external engine variables). A series of experiments conducted at widely separated points in the operating range of the engine have confirmed that the transient accuracy of the model is comparable to its steady state accuracy. The basic model includes a description of the emissions to be expected during transient engine operation: NO_x, HC, CO and CO_2. The emission submodels have been validated in a way similar to the mechanical subsystems though their accuracy is slightly less, ±5%.

Given the accuracy of the model and the fact that all of the results presented where obtained using a PC–AT, the basic model can be seen as an inexpensive engineering tool having wide applications to engine control problems. The model has also shown itself to be a useful teaching tool and thus is applicable to "expert system" application due to its minimal format.

Work is currently underway to construct model based control systems using the mean value engine model. This includes a condition monitoring facility as the model is obviously capable of "looking inside" an operating engine with only the sensors currently used for control.

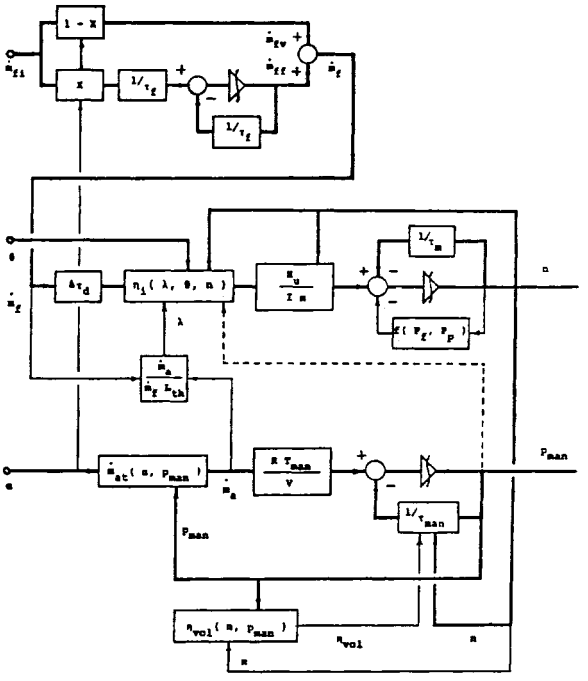

Figure 5. Nonlinear block diagram of the CFI four–cycle spark ignition mean value engine model. On the left are the engine control inputs while on the engine outputs are on the right. The block diagram has been drawn to emphasize the three main dynamic subsystems: each includes an integrator. The time constants shown are the large signal time constants (see text).

6. Nomenclature

t	time (sec)
p_{amb}	ambient pressure (bar)
T_{amb}	ambient temperature (degrees kelvin)
α	throttle plate angle (degrees)
$\dot{m}_{at}$	air mass flow rate past throttle plate (kg/sec)
$\dot{m}_{fi}$	injected fuel mass flow (kg per sec)
$\dot{m}_f$	cylinder port fuel mass flow (kg per sec)
$\dot{m}_{ff}$	fuel film mass flow (kg per sec)
$\dot{m}_{fv}$	fuel vapor mass flow (kg per sec)
X	fraction of the injected fuel which is deposited

Figure 6a. Measured throttle angle during tip–in/–out experiment. This is also the model input for the simulation experiment.

Figure 6b. Calculated and measured manifold air pressure for the input above.

Figure 6c. Calulated and measured air mass flow for the transient model test.

Figure 6d. Measured fuel flow and model input corresponding to the throttle angle transient above.

Figure 6e. Lambda sensor measurement compared to the calculated model result.

Figure 6f. Calculated and measured crank shaft speed for the throttle angle pulse experiment above.

	on manifold as fuel film
L_{th}	stoichiometric air/fuel mass ratio for gasoline (14.67)
λ	air/fuel equivalence ratio = $\dot{m}_{at}/(\dot{m}_f L_{th})$
p_{man}	manifold air pressure (bar)
T_{man}	manifold air temperature (degrees Kelvin)
p_{exh}	exhaust pressure (bar)
θ	spark advance angle (degrees)
η_i	indicated efficiency
η_{vol}	volumetric efficiency (based on intake pressure)
η_{vamb}	volumetric efficiency (based on ambient pressure)
n	crank shaft speed (rpm)
I	total moment of inertia loading engine (kg m²/1 kW)
P_f	frictional power (kW)
P_P	pumping power (kW)
P_b	load power (kW)
H_u	fuel heating value (kJ/kg)
V_d	engine displacement (m^3 or liters)
V	manifold + port passage volume (m^3)
R	gas constant
κ	ratio of the specific heats = 1.4 for air
c_t	flow coefficient of throttle body throat
D	diameter of throttle body throat (m)

7. References

1. Rasmussen, I., Emissioner fra Biler (In Danish, Emissions from Cars), Ph. D. Dissertation, Laboratory for Energetics, The Technical University of Denmark, 1976.

2. Melgaard, H., Hendricks, E. and Madsen, H., "Parameter Estimation and Condition Monitoring of Spark Ignition Engines.", to be published, 1990 ACC.

3. Hendricks, E. L. and Sorenson, S. C., "Mean Value Modelling of Spark Ignition Engines, SAE Technical Paper 900616, 1990.

4. Taylor, C. F., and Taylor, E. S., The Internal Combustion Engine, Second Edition, Int. Textbook Co., Scranton, Pa., 1970.

5. Sorenson, S., FLOSIM, Laboratory for Energetics, Technical University of Denmark, Lyngby, Denmark, 1988.